Antivirals & Antiretrovirals

Jones et al., J Antivir Antiretrovir 2014, 6:3
http://dx.doi.org/10.4172/jaa.1000101

Research Article Open Access

Preclinical and Clinical Profile of HIV-1 Integrase Strand-transfer Inhibitor GS-9224 Compared to its Parent Compound GS-9160

Gregg S Jones, Rebecca Hluhanich, Lani M Wieman, Jim Zheng, Wayne Huang, April Kinkade, Eugene J Eisenberg, Chris Yang, Damian McColl, Anita Mathias, Haolun Jin, Tomas Cihlar, Matthew Wright, Romas Geleziunas and Manuel Tsiang*

Gilead Sciences, Foster City, CA 94404, USA

Abstract

In an effort to optimize the pharmacokinetic profile of GS-9160, a potent (EC_{50}=1.2 – 4 nM) antiviral tri-cyclic HIV-1 integrase (IN) strand transfer inhibitor (INSTI), various substitutions on the p-fluorobenzyl moiety of GS-9160 were explored. This effort led to the discovery of GS-9224, an analog containing a 5-chloro-2,4-di-fluorobenzyl moiety. GS-9224, like its predecessor GS-9160, has potent (EC_{50}=1.3 – 9 nM) and selective antiviral activity against HIV-1 and acts as a bona fide integration inhibitor through elevation of 2-long terminal repeat (2-LTR) circles and decrease of integration junctions in HIV-1 infected cells, markers of failed viral integration. Viral resistance selections with GS-9224 yielded three mutations within the catalytic core domain of HIV-1 IN: G140S, L74M and Q148K. When tested against a panel of HIV-1 clones engineered to express INSTI resistance mutations, the profile of GS-9224 was comparable to GS-9160. GS-9224 exhibits improved hepatic microsome stability, better absorption potential and a lower *in vitro* intestinal efflux ratio compared to GS-9160. In addition, GS-9224 displayed higher dog plasma protein binding (~99%) than GS-9160 (~93%) suggesting a potential for protein restricted clearance. However, the improved metabolic stability, absorption potential and serum protein binding of GS-9224 compared to GS-9160 did not translate into an improved clinical pharmacokinetic profile. Results from a single-dose study in human healthy subjects revealed a fast systemic clearance of GS-9224 with a terminal half-life of ~ 1 h, resulting in a pharmacokinetic profile that would not support once-daily dosing in HIV-infected patients.

Keywords: HIV-1; GS-9224; GS-9160; Strand-transfer

Introduction

As an essential enzyme for HIV-1 replication, integrase (IN) is an attractive target for antiviral drug discovery. During the viral life cycle, the primary function of IN is to catalyze the insertion of reverse-transcribed double stranded HIV-1 DNA into the host cell genome to establish the provirus. Inhibition of the strand transfer activity of IN as a target for therapeutic intervention is now well validated clinically [1,2]. Raltegravir (RAL) was the first IN strand-transfer inhibitor (INSTI) to be approved for clinical use and is dosed twice daily [3-5]. Elvitegravir (EVG) is co-administered with cobicistat, a new pharmacokinetic enhancer that enables once-daily dosing of EVG [6-8]. A once-daily single tablet regimen (STRIBILD™) containing EVG, cobicistat, deoxyfluorothiacytidine (FTC) and tenofovir disoproxil fumarate (TDF) has been recently approved by the FDA for the treatment of HIV infection. In two Phase III studies, the STRIBILD regimen showed non-inferior efficacy and safety in treatment-naïve HIV-infected patients when compared head-to-head with either efavirenz [9] or atazanavir [10] containing once-daily treatment regimens. Recent data from the 96-week extension analysis of both studies established the longer term durability and efficacy of the STRIBILD regimen [11,12].

Specific mutations in IN conferring cross-resistance to RAL and EVG have been identified in clinical settings [13-15]. The INSTI dolutegravir (S/GSK1349572), which is dosed once-daily without boosting, displayed a resistance profile that is distinct from those of RAL and EVG [16,17]. In phase III clinical studies, none of the subjects treated with the combination of dolutegravir and TDF/FTC for up to 48 weeks developed any treatment-associated IN mutations [18].

In an effort to identify additional novel INSTIs that could be dosed once-daily without pharmacokinetic enhancement we explored modifications of a tricyclic analog GS-9160, a potent and orally bioavailable compound [19-21]. Substitutions on the p-fluorobenzyl moiety of GS-9160 led to the discovery of GS-9224, which contains a 5-chloro-2,4-di-fluorobenzyl moiety [22]. In this report, we describe detailed biological and metabolic characterization of GS-9224 including a clinical pharmacokinetic profile in healthy human volunteers.

Materials and Methods

Compounds

GS-9224 and GS-9160 were synthesized at Gilead Sciences, Inc. L-870,810 was synthesized by Combi Blocks, Inc. (San Diego, CA). RAL was synthesized by Naeja Pharmaceuticals, Inc. (Edmonton, Alberta Canada). All three compounds have a purity of >95% as determined by analytical reversed phase HPLC using a Phenomenex Luna C18 column and UV detection at 214 nm and 254 nm. The structures of these three INSTIs are shown in (Figure 1).

Cells

MT-2 cells were obtained from Stanford University and MT-4 cells were obtained from the NIH AIDS Research and Reference Reagent Program (Germantown, MD). SupT1 cells were obtained from the American Type Culture Collection (Rockville, MD). MT-2, MT-4 and SupT1 cells were maintained in RPMI-1640 medium (Cat # 61870-

***Corresponding author:** Manuel Tsiang, Gilead Sciences, 333 Lakeside Drive, Foster City, CA 94404, USA, Tel: (650) 522-5860; Fax: (650) 522-5143; E-mail: MTsiang@gilead.com

Received June 04, 2014; **Accepted** July 10, 2014; **Published** July 18, 2014

Citation: Jones GS, Hluhanich R, Wieman LM, Zheng J, Huang W, et al. (2014) Preclinical and Clinical Profile of HIV-1 Integrase Strand-transfer Inhibitor GS-9224 Compared to its Parent Compound GS-9160. J Antivir Antiretrovir 6: 075-083. doi:10.4172/jaa.1000101

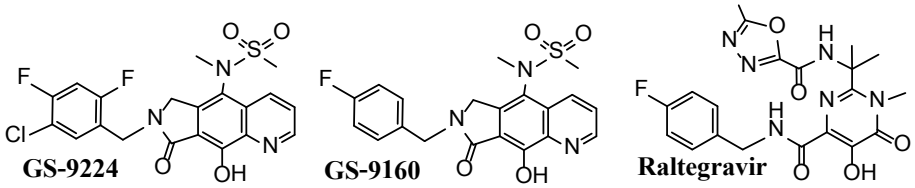

Figure 1: Structures of integrase strand transfer inhibitors.

036, Life Technologies, Grand Island, NY) supplemented with 10% heat-inactivated fetal bovine serum (FBS) (Cat # SH30071.03, GE Healthcare Sciences, Logan, UT) and antibiotics. Peripheral blood monocytes (PBMCs) were isolated from the buffy coats of healthy human volunteers (Stanford Medical School Blood Center, Stanford, CA).

Viruses

HIV-1 strain IIIb was obtained from Advanced Biotechnologies Inc. (Columbia, MD). The NRTI-resistant virus containing mutation K65R in reverse transcriptase (RT) was obtained from Mark Wainberg (McGill AIDS Center, Montreal, Canada). The NRTI-resistant virus RT-M184V and NNRTI-resistant viruses RT-K103N and RT-Y181C were constructed by site-directed mutagenesis [23]. The NRTI-resistant virus, RT-6TAMs (M41L, D67N, K70R, L210W, T215Y and K219Q) which confers resistance to thymidine analogs [23] as well as the protease (PR) inhibitor-resistant viruses, PR-I84V/L90M and PR-G48V/V82A/L90M were constructed by homologous recombination in electroporated SupT1 cells [24]. All the above mutant viruses were constructed from an HXB2 clone.

Construction of infectious HIV-1 DNA clones with IN mutations

Mutations conferring resistance to INSTI were introduced into the infectious HIV-1 DNA clone HXB2 by site-directed mutagenesis at Gilead Sciences by our investigators [19]. Briefly, the 15.5 Kb HXB2 plasmid DNA was cut with ApaI and SalI to generate a 3.7 Kb ApaI – SalI fragment that was gel-purified. This 3.7 Kb fragment containing both the RT and the IN coding regions was then subcloned into pUNI/V5-His B (Invitrogen, Carlsbad, CA) to generate pHXB2 (3.7). Mutations were selectively introduced into integrase using the Quick change Site-Directed Mutagenesis Kit (Stratagene, La Jolla, CA) to generate the mutagenized clones, pHXB2(3.7) mut. After confirmation of the mutation(s) by sequencing, DNAs were prepared from the pHXB2(3.7) mut clones and the ApaI - SalI fragment containing the integrase mutation(s) was isolated for subcloning back into HXB2 by replacement of the wild-type 3.7 Kb ApaI – SalI fragment.

IN strand-transfer assay

Expression and purification of recombinant IN containing an N-terminal 6His-tag has been described in the materials and methods section of an earlier study conducted at Gilead Sciences by our investigators [19]. The strand transfer assay was described in detail in the experimental procedures section of an earlier study conducted at Gilead Sciences by our investigators [25]. Briefly, biotinylated donor DNA was bound to streptavidin coated plates. Unbound donor DNA was removed by washing, and IN was then added to each well to allow 3'-processing of the donor DNA end for 30 min. Digoxigenin-tagged target DNA was next added to each well, and the 3'-end-joining reaction was allowed to proceed for 30 min. The wells were washed to remove un-joined target DNA, and the chemiluminescence signal was detected following addition of horseradish peroxidase-conjugated anti-digoxigenin antibody. Test compounds were added immediately before the target DNA.

Antiviral and cytotoxicity assays

Antiviral and cytotoxicity assays in HIV-1 IIIb infected MT-2, MT-4 and SupT1 cells and PHA plus IL-2 stimulated human PBMCs have been described in the materials and methods section of an earlier study by our investigators at Gilead Sciences [19]. Briefly, for the antiviral assay utilizing MT-2 and MT-4 cells, 50 µL of 2X test concentration (total of 9 concentrations) of 3-fold serially diluted compound in culture medium with 10% FBS was added to each well of a 96-well plate in triplicate. MT-2 cells were infected with HIV-1 IIIb virus at a multiplicity of infection (MOI) of ~0.01 for 3 hours at 37°C. Fifty microliters of infected cell suspension in culture medium with 10% FBS (~1.5 x 10^4 cells) was then added to each well containing 50 µL of diluted compound. The plates were then incubated at 37°C for 5 days. At the end of the incubation, 100 µL of CellTiter-Glo™ Reagent (catalog # G7571, Promega Biosciences, Inc., Madison, WI) was added to each well. Cell lysis was carried out by incubating the assay plates at room temperature for 10 min followed by the quantification of chemiluminescence signal using the Envision plate reader (Perkin Elmer, Shelton, CT). For compound cytotoxicity assessment in MT-2 and MT-4 cells, a protocol identical to that of the antiviral assay was followed, except that uninfected cells were used and a higher concentration range of compound was tested.

To study the effect of serum proteins on the antiviral activity of INSTI, compounds were tested in the presence of either 35 mg/ml HSA (catalog #A-1653, Sigma, St. Louis, MO), or 1.5 mg/ml α_1-AGP (catalog #G-9885, Sigma, St. Louis, MO). To assess the effect of human serum on compound potency, the assay was performed in the presence of 10%, 20%, 35% and 50% human serum from clotted whole blood (catalog #14-498E, Cambrex Bio Science, Walkersville, MD).

2-LTR circle accumulation assay

The assay for 2-LTR circle accumulation was adapted from a previously described method [26]. SupT1 cells were infected in bulk culture with HIV-1 IIIb at a multiplicity of infection (MOI) of 10 and at a cell density of 4 × 10^6 cells/ml for 3 hours at 37°C. We have confirmed in a time course experiment in our own system a previous observation that 2-LTR circles reached a peak production 24 hours post-infection [26]. For this reason, measurement of 2-LTR circles was performed at 24 hours post-infection in our inhibition dose response studies. Both the 2-LTR junction (2-LTR circles) and the host globin gene (used to normalize for cell number) were quantified using Taqman real-time PCR [19]. The copy number of 2-LTR circles was normalized to that of the globin gene and plotted against drug concentration for EC_{50} determination.

Alu-PCR Assays

The Alu-PCR assay has been previously described [26]. MT-2 cells were infected as a bulk culture with pseudotyped HIV-1 vector particles produced from the SODk1 2G cell line [26,27] at an m.o.i. of 10 and a cell density of 4×10^6 cells/ml for 3 hours at 37°C. The plates were incubated at 37°C for 12 hours for Late-RT product quantification and for 48 hours for Alu-PCR product quantification. The levels of Late-RT sequences and integration junctions quantified at 12 and 48 hours post-infection respectively were normalized to the level of globin gene present in the sample at these time points. Quantification by PCR was performed on the ABI Prism® 7900HT Sequence Detection System (Applied Biosystems, Foster City, CA).

Data analysis

The entire curve fitting to generate EC_{50} and CC_{50} as well as error calculations were performed using Sigma Plot scientific data analysis and graphing software (Systat Software Inc., San Jose, CA).

Viral resistance selection

Resistance selections were carried out in 6-well tissue culture plates. MT-2 cells were seeded at a density of 0.5×10^6 cells per well in 5 ml of culture medium. Compounds were added at a final concentration corresponding to their antiviral EC_{50} or twice the EC_{50}. HIV-1 IIIb was used at an MOI of ~ 0.01. The cultures were incubated at 37°C and split 1/2-1/3 once or twice a week depending on the growth status of the cells. Cytopathic effect (CPE) manifested as syncytia formation was used to follow progression of infections. Virus was harvested and transferred to fresh MT-2 cells in the presence of higher concentrations of compounds. Successive viral passages were obtained by repeating this procedure. The duration of each passage ranged from 10-15 days.

Population and clonal sequencing of HIV-1

Viral RNA isolated from culture supernatants was used for cDNA synthesis. Five µl of cDNA was used for PCR amplification of a 2765 base pair fragment spanning nucleotide 372 of the RT coding region to nucleotide 127 of the vpr gene and encompassing the entire IN open reading frame. The following primers were used for PCR: pLAIF3004: 5'–CAGGAAGTATACT GCATTTACC–3' and pLAIR5768: 5'–CTAAGCCATGGAGCCAAATCC–3' (Bio Source International, Foster City, CA). The PCR product was purified using the QIA quick PCR purification kit (Catalog #28104, QIAGEN, Valencia, CA). This PCR product was used for population sequencing of drug-resistant viral pools and both DNA strands were sequenced (ELIM Biopharmaceuticals Inc, Hayward, CA). For clonal sequencing, a 1296 base pair PCR product spanning nucleotide 1608 of the RT coding region to nucleotide 412 of the vif gene was used as template. The PCR product was purified on a 1.0% agarose gel and cloned into the pCR-Blunt II-TOPO plasmid using the Zero Blunt TOPO PCR Cloning Kit (Catalog #K2800-20, Invitrogen, Carlsbad, CA). Thirty transformed bacterial colonies were picked and cultured overnight in L-Broth containing 50 µg/ml kanamycin. Plasmid DNAs were isolated using a Wizard SV 96 Plasmid purification kit (Catalog #A2255, Promega, Madison WI) and sequenced through the IN region on both DNA strands (ELIM Biopharmaceuticals Inc, Hayward, CA) using the following primers: INTseq14157: 5'–ACCAGCACACAAAGGAATTGG–3' and VIFseq2Rev5453: 5'–CCTGCTTGATATTCACACC–3' (BioSource International, Foster City, CA).

Hepatic microsomal stability assay

Microsome (MS) suspensions were prepared by dilution of stock microsomes (In Vitro Technologies, MD) with 0.05 M phosphate buffer, pH 7.4 to obtain protein concentrations of 0.5 mg/mL. Compounds were mixed with MS suspension media (pre-heated for 5 min at 37°C) and cofactors were added to start the reaction. The final reaction mixture contained: 2 µM compound, 0.5 mg/mL microsomal protein, 1.25 mM NADPH, 3.3 mM $MgCl_2$ and 0.05 M phosphate buffer, pH 7.4. At 0, 5, 15, 30, 45 and 60 min, 25 µL of the reaction mixture were quenched with 250 µL of internal standard (50 nM)/mobile phase B. The analytical internal standard was suspended in 0.2% formic acid/95% acetonitrile/5% water. After quenching, the plates were centrifuged at 3000 × g for 10 min. Five µL samples were analyzed by LC/MS/MS (LOQ = 0.001µM). Verapamil was used as a positive control for microsomal activity.

Caco-2 permeability

Caco-2 cells were grown to confluence on 24 well PET (polyethylene-terephthalate) plates (BD Biosciences, San Jose, CA). Donor HBSS buffer from Invitrogen was supplemented with 10 mM HEPES and 15 mM glucose with pH adjusted to pH 6.5. Receiver HBSS buffer was supplemented with 1% BSA with pH adjusted to pH 7.4. After equilibration with transport buffer, trans-epithelial electrical resistance was measured to confirm membrane integrity. The assay was initiated by the addition of compound containing buffer to the donor compartment. Samples of 100 µL were removed from the receiver compartment at 1 and 2 h post compound addition. The removed samples were immediately mixed with 400 µL of 0.1% formic acid in acetonitrile to precipitate protein and stabilize test compounds. Cells were dosed on either the apical or baso-lateral side to determine the forward (A to B) and reverse (B to A) permeability. Permeability through the membrane and non-specific binding was measured through a cell free trans-well. To test for non-specific binding and compound instability, the total amount of compound was quantified at the end of the experiment and compared to the material present in the original dosing solution to determine % recovery. Samples were analyzed by LC/MS/MS.

Plasma protein binding assay

Equilibrium dialysis was conducted at 37°C using Beagle dog and human plasma containing either GS-9224 or GS-9160 at the final concentrations of 2 µM. Based on a pilot time-to-equilibrium study and stability data, a 30-hour dialysis time was chosen for plasma protein binding determinations. Prior to the study, dialysis membranes were soaked for approximately one hour in 0.133 M phosphate buffer, pH 7.4. Plasma samples containing compound (1 mL) and compound-free phosphate buffer (1 mL) were placed into opposite sides of the assembled dialysis cells. The dialysis cells were rotated slowly in a 37°C water bath for 30 h. Plasma samples were next drained into pre-weighed polypropylene tubes containing 1 mL of phosphate buffer. Buffer samples were drained into pre-weighed tubes containing 1.0 mL of blank plasma of the matching species. Post-dialysis plasma and buffer weights were measured and recorded for calculations.

Pharmacokinetic profiling in healthy human subjects

Ten healthy subjects were randomized to receive a single dose of GS-9224 (n=8) or matching placebo (n=2) following an overnight fast. Doses of 50 and 100 mg were administered in orange juice on day 1 and day 9 to the same patients (including a rinse of the dispensing container) to a total liquid volume of 240 mL with dosing within 15 minutes of study drug preparation. Following study drug administration, subjects were restricted from water intake until after the 2-hour blood draw and

from food intake until after collection of the 4-hour blood draw. Serial blood samples were collected at times: 0 (predose), 0.25, 0.5, 0.75, 1, 1.5, 2, 2.5, 3, 3.5, 4, 5, 6, 8, 10, 12, 18, 24, 28, 32, 36, 40, 44, and 48 hours postdose. In subjects that received GS-9224 plasma concentrations were measured at all-time points; protein binding of GS-9224 was assessed at the 1-hour time point.

Assessment of adverse events and concomitant medications continued throughout the duration of the study. Laboratory analysis, serial ECGs, and physical examinations were performed at screening, at defined intervals during the confinement periods, and at the follow-up evaluation 7 days after the last dose of study drug administration.

The study protocol and informed consent document(s) were reviewed and approved by the study center's Institutional Review Board and subjects were provided written informed consent before study participation. The studies were carried out in accordance with the clinical research guidelines established by the Basic Principles defined in the U.S. 21 CFR Part 312.20 and the principles enunciated in the latest version of the Declaration of Helsinki.

Results

GS-9224 exhibits potent antiviral activity and is synergistic with HIV antiviral drugs

In an effort to improve the pharmacokinetic profile of previously published INSTI GS-9160 [19-21], various substitutions on the p-fluorobenzyl moiety of GS-9160 were explored leading to the discovery of the close analog GS-9224 containing a 5-chloro-2,4-fluorobenzyl moiety (Figure 1) [22].

The antiviral activity of GS-9224 was evaluated in HIV-1 infected MT-2 and MT-4 cell lines as well as in primary human PBMCs (Table 1). The anti-HIV activity of GS-9224 was similar in all three cell types with an EC_{50} range of 1.3 to 9 nM. This potency is within a range similar to that observed for RAL and slightly lower than the parent analog GS-9160. To assess the impact of human serum protein binding on the antiviral potency of GS-9224 and to provide a target trough concentration in humans to achieve efficacy, the antiviral activity of GS-9224 was determined in the presence of human serum and the human serum components including human serum albumin (HSA) and α_1-acid glycoprotein (α_1-AGP) (Table 2). The EC_{50} of GS-9224 in 100% human serum was extrapolated from the EC_{50} values determined in the presence of 10, 20, 35 and 50% human serum. The combined effect of both serum proteins, HSA and α_1-AGP increased the EC_{50} of GS-9224 by ~14.6-fold in MT-2 cells, while the EC_{50} values of GS-9160 and RAL were increased by 10.8- and 3-fold, respectively. Whole human serum had an effect similar to the combined serum proteins in MT-2 cells and increased the EC_{50} of GS-9224 by 12.3-fold. In human PBMCs, the combined effect of HSA and α_1-AGP increased the EC_{50} of GS-9224 by 8.6-fold, a similar shift in the EC_{50} values as that observed for GS-9160 and RAL (10.8- and 7.3-fold, respectively).

Similar to GS-9160, GS-9224 showed synergistic antiviral effect in HIV-1-infected MT-2 cells when combined with approved drugs from different antiretroviral classes including PIs (lopinavir, atazanavir, and nelfinavir), NNRTIs (efavirenz) and N(t)RTIs (tenofovir, zidovudine, emtricitabine, and lamivudine) (Table S1).

GS-9224 inhibits HIV-1 integrase function and integration in infected cells

The inhibitory effect of GS-9224 on IN enzymatic activity was evaluated in a biochemical assay that measures the activity of IN in an *in vitro* integration reaction mediating the strand transfer of viral donor DNA unto host or target DNA. GS-9224 produced inhibitory activity (IC_{50} = 55 nM) that was comparable to that of GS-9160 (IC_{50} = 29 nM) and RAL (IC_{50} = 34 nM) (Table 3). An elevation in the levels of circular HIV DNA species containing 1- or 2-long terminal repeats (1-LTR and 2-LTR circles) following the treatment of infected cells with a small molecule can provide evidence that HIV integration has been inhibited [28]. Treatment of HIV-1 infected SupT1 cells with GS-9224 caused a ~3.9-fold increase in 2-LTR circles. The effect was dose-dependent with an EC_{50} of 9.5 nM (Table 3). Similar results were obtained with the parental analog of GS-9224, GS-9160 and the clinically validated integrase strand-transfer inhibitor, RAL. This result provided initial evidence that GS-9160 can block HIV-1 integration in a cell.

Another method to assess whether HIV-1 integration is inhibited in infected cells is by direct measurement of integration junctions between HIV proviral DNA and the host chromosomal DNA [26]. Detection by PCR of nucleic acid products containing Alu-repeat sequences

Compound	Anti-HIV in MT2[a]	Cytotoxicity in MT2[a]	Anti-HIV in MT4[a]	Cytotoxicity in MT4[a]	Anti-HIV in PBMC[b]	Cytotoxicity in PBMC[b]
	EC_{50} (nM)	CC_{50} (nM)	EC_{50} (nM)	CC_{50} (nM)	EC_{50} (nM)	CC_{50} (nM)
GS-9224	1.3 ± 1.1	1600 ± 600	9.4 ± 0.5	700 ± 300	5 ± 6	5850 ± 900
GS-9160	1.2 ± 0.5	4200 ± 1000	4 ± 3	800 ± 400	1.2 ± 0.9	3880 ± 1700
RAL	7.5 ± 1	>100,000	8 ± 2	58200 ± 7300	2.6 ± 1.2	210,500 ± 90,000

[a] Mean ± SD of at least 4 independent experiments.
[b] Mean ± SD of at least 3 different donors.

Table 1: Antiviral Activity of GS-9224 in Various HIV-1 Infected Human Cell Types.

Compound	Anti-HIV in MT2 Cells					Anti-HIV in Human PBMCs		
	10% FBS[a,b]	10% FBS + HSA + α_1-AGP[b]		100% HS[d]		10% FBS[a,c]	10% FBS + HSA + α_1-AGP[c]	
	EC_{50} (nM)	EC_{50} (nM)	EC_{95} (nM)[e]	EC_{50} (nM)	EC_{95} (nM)[e]	EC_{50} (nM)	EC_{50} (nM)	EC_{95} (nM)[e]
GS-9224	1.3 ± 1.1	19 ± 5	118 ± 28	16	100	2.2 ± 0.1	19 ± 6	121 ± 39
GS-9160	1.2 ± 0.5	13 ± 6	76 ± 35	12	75	1.2 ± 0.9	13 ± 13	80 ± 79
RAL	7.5 ± 1	23 ± 5	162 ± 35	–	–	2.6 ± 1.2	19 ± 14	121 ± 93

[a] The EC_{50} for Control (10% FBS) and (10% FBS + HSA + α_1-AGP) were run in parallel.
[b] Mean ± SD of at least 3 independent experiments.
[c] Mean ± SD of at least 3 donors.
[d] Mean of at least 2 independent experiments.
[e] The values of EC_{95} were calculated from EC_{50}.

Table 2: Effect of Serum Proteins on the Antiviral Activity of GS-9224.

Compound	Strand Transfer[a]	2LTR Circles in SupT1[b]		Cytotoxicity in SupT1[c]	Late RT in MT-2[b]	Alu-LTR in MT-2[b]	Cytotoxicity in MT-2[c]
	IC_{50} (nM)	Maximum Fold-Change	EC_{50} (nM)	CC_{50} (nM)	EC_{50} (nM)	EC_{50} (nM)	CC_{50} (nM)
GS-9224	55 ± 10	3.9 ↑	9.5	2600	>100	2.8	1600
GS-9160	29 ± 3	2.3 ↑	11	970	>100	1.8	4200
RAL	34 ± 5	2.4 ↑	12	>100,000	>200	3.6	>100,000
EFV	–	0.2 ↓	1.5	14000	3.5	1.3	>27,000
APV	–	1 ↔	–	83000	>500	>500	>50,000

[a] Mean ± SE of at least 4 independent experiments using IN enzyme.
[b] Mean of at least 2 independent experiments in HIV-1 infected SupT1 or MT-2 cells.
[c] Mean of at least 4 independent experiments in uninfected SupT1 or MT-2 cells.

Table 3: Inhibition of Integrase Enzymatic Strand Transfer Activity and Integration in HIV-1 Infected SupT1 and MT-2 Cells.

Compounds[j]	EC_{50} (nM)	Fold-Change in EC_{50} Relative to HIV-1 IIIb												
	HIV-1 IIIb	T66I[a]	L74M[b]	E92Q[c]	E92V[d]	E138K[e]	Q148K[f]	V151A[g]	N155H[h]	N155S[i]	L74M/ E92V	E92V/ V151A	E138K/ Q148K	E92V/ G140S/ V151A
RAL	4.3	1.9	1.7	6	7	1	136	4	24	43	15	31	747	166
GS-9160	1.7	1.9	1	26	17	1	28	10	61	36	56	126	676	689
GS-9224	5.6	1	1	21	7	1	42	5	110	65	25	73	419	438

> 2-fold > 10-fold > 50-fold > 100-fold > 400-fold

[a] Selected by L-708,906 (30, 32), S-1360 (31, 33) and EVG (37).
[b] Selected by GS-9224 (this report), L-708,906 (32), S-1360 (33), L-870,810 (42) and GS-9160 (19).
[c] Selected by EVG (31) and L-870,810 (42).
[d] Selected by GS-9160 (19).
[e] Selected by S-1360 (33).
[f] Selected by GS-9224 (this report), S-1360 (31) and RAL (14, 39).
[g] Selected by GS-278012, an analog of GS-9160 (19).
[h] Developed in SHIV (89.6P) infected Rhesus macaques treated with L-870,812 (34).
[i] Selected by S-1360 (31).
[j] The EC_{50} and fold-change represent the mean of a least two independent experiments performed in triplicate.

Table 4: Resistance Profile of Mutant Viruses Conferring Resistance to INSTIs.

and portions of HIV-1 DNA represents a marker of successful HIV-1 integration. These products typically peak at 48 hours post-infection. In the presence of GS-9224, these products decreased in a dose-dependent manner with an EC_{50} of 2.8 nM, an activity comparable to that observed with GS-9160 and RAL in the same assay (Table 3). To ensure that this reduced integration was not attributable to an impairment of the upstream process of reverse transcription, accumulation of late RT products was assessed in the presence of GS-9224. GS-9224, like the other two strand-transfer inhibitors, GS-9160 and RAL did not affect the accumulation of late reverse transcription products which were in sharp contrast to the inhibitory effect noted with the NNRTI efavirenz (Table 3). This result provides unequivocal evidence that GS-9224 acts as an authentic inhibitor of integration in HIV-1 infected cells.

GS-9224 is active against drug-resistant mutants of HIV-1

The antiviral activity of GS-9224 was determined against a panel of drug-resistant mutants of HIV-1. The panel included mutants that were resistant to N(t)RTIs (K65R, M184V and TAMs), NNRTIs (K103N and Y181C) and PIs (I84V/L90M and G48V/V82A/L90M). GS-9224, like GS-9160 and RAL, retained activity against all NRTI-, NNRTI- and PI-resistant mutants tested (Table S2). The antiviral activity of GS-9224 against these drug-resistant mutants was comparable to its activity against the wild-type reference virus HIV-1 IIIb (Table 1).

Activity of GS-9224 against viruses with mutations conferring resistance to other INSTIs

Resistance mutations previously selected with other INSTIs [14,29-42] were introduced into an HIV-1 infectious molecular clone to determine if they confer cross-resistance to GS-9224 (Table 4). The T66I and L74M mutant viruses showed no resistance against GS-9224, GS-9160 or RAL. E92Q displayed comparable resistance to GS-9224 and GS-9160 (~20-fold) but lower resistance to RAL (~6-fold). Similarly, N155H conferred higher levels of resistance to GS-9224 and GS-9160 (~60–100-fold) compared to RAL (~24-fold). In contrast, Q148K appears to have a complementary resistance pattern to that of E92Q and N155H, displaying a higher level of resistance to RAL (>100-fold). E138K alone does not contribute any resistance to GS-9224 and the other INSTIs, but it greatly enhanced the resistance to all INSTIs tested when combined with Q148K. In summary, the resistance pattern of GS-9224 is similar to that of GS-9160, but somewhat distinct from that of RAL.

In vitro resistance selection in the presence of GS-9224

Serial passaging of HIV-1 IIIb virus in MT-2 cells in the presence of increasing concentrations of GS-9224 (Figure 2) led to the emergence of a virus pool displaying a 4.6-fold resistance to GS-9224 by passage 4 and >100-fold resistance by passage 6 (Table 5). The viruses selected with GS-9224 displayed similar levels of cross-resistance to RAL both at passage P4 and P6, but remained fully sensitive to compounds from other antiretroviral classes.

GS-9224 Selected a different pattern of INSTI resistance mutations than GS-9160

Population sequencing of GS-9224-selected viral passages revealed the successive emergence of mutations G140S, L74M and Q148K in the catalytic core domain of HIV-1 IN (Figure 2). Clonal sequencing of passage 4 revealed that G140S and L74M are each present in 62% of the clones, suggesting that at least 24% of the clones carried both mutations. Both G140S and L74M were present in 100% of the clones sequenced at passage 6 while Q148K, a third mutation which appeared in passage 6 was present in 93.3% of the clones. The S24G mutation which was detected by population sequencing of passage 5 virus is

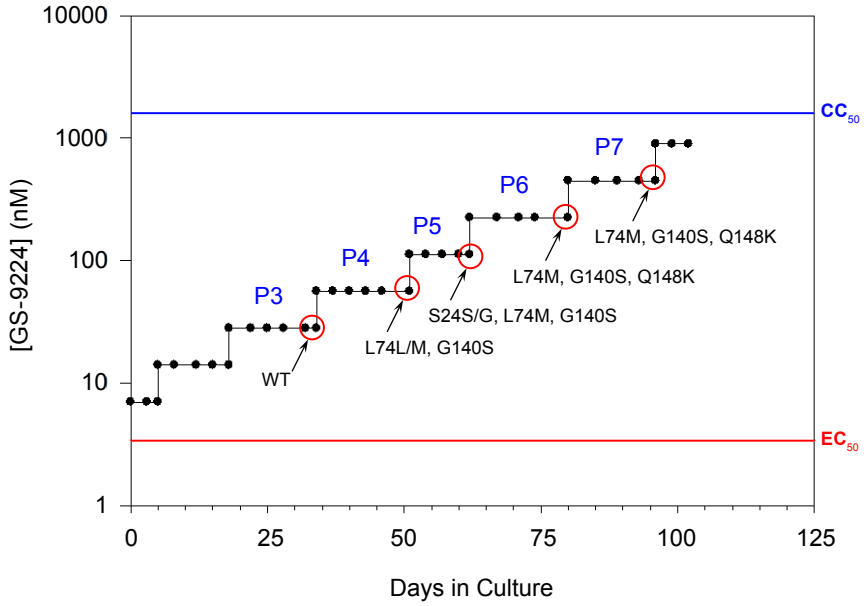

Figure 2: Progress of resistance selection and and emergence of resistance mutations selected in vitro in the presence of GS-9224. The EC_{50} and CC_{50} values of GS-9224 in MT-2 cells are indicated by the red and blue lines respectively. Each closed black circle represents one passage of the infected cell culture. Viral passages 3, 4, 5, 6 and 7 are denoted as P3, P4, P5, P6 and P7 and represent a transfer of cell-free virus supernatant to fresh uninfected cell culture with a doubling of the drug concentration. The culture supernatant from the last infected cell culture before the increase of inhibitor concentration (red circle) was used for population sequencing and the mutations identified in the integrase region are indicated. In addition, P4 and P6 viral pools were used for clonal sequencing to determine the percentage of clones containing each identified mutation. P4 virus: L74M (62%), G140S (62%); P6 virus: L74M (100%), G140S (100%), Q148K (93.3%).

Compound	EC_{50}, nM (fold change relative to HIV-1 IIIb)		
	HIV-1 IIIb[a]	GS-9224 P4 Virus[b]	GS-9224 P6 Virus[b]
TFV	3.8 ± 0.8	3 ± 0.4 (0.9)	5.9 ± 0.9 (1.6)
EFV	0.7 ± 0.1	1.3 ± 0.2 (1.9)	1.5 ± 0.3 (2.2)
LPV	13.0 ± 4.0	27.0 ± 6.0 (2.1)	20.9 ± 0.8 (1.6)
RAL	3.5 ± 0.6	11.0 ± 1.2 (3.1)	237.0 ± 126.0 (>100)
GS-9224	4.0 ± 2.0	18.6 ± 2.7 (4.6)	>1000 (>100)

[a] Mean ± SD of at least 6 independent experiments.
[b] Mean ± SD of at least 3 independent experiments.
The numbers in parentheses represent the fold-change over wild-type virus.

Table 5: Resistance Phenotype of GS-9224 Selected Viral Pools.

a known natural polymorphism of IN that is not associated with resistance to INSTIs [43]. In fact, by passage 6, this mutation was no longer detectable. Since the level of resistance increased from 4.6-fold to >100-fold from passages 4 to 6 with the appearance of the additional mutation Q148K, we wished to determine whether combining IN mutations L74M, G140S and Q148K in a molecular clone of HIV-1 would recapitulate resistance to GS-9224. These mutations were introduced either individually or together into an infectious molecular clone of HIV-1. Interestingly, as individual mutations, Q148K conferred 42-fold resistance to GS-9224, L74M alone had no effect and G140S alone conferred 6-fold resistance (Table 6). When L74M and G140S were combined, the double mutant conferred 11-fold resistance, suggesting that L74M may potentiate resistance conferred by G140S, a property of L74M that we previously reported with regard to the E92V mutation [19]. Notably, the triple mutant L74M/G140S/Q148K conferred >100-fold resistance to GS-9224, a level consistent with that observed for passage 6 virus (Tables 5 and 6). All combinations of the tested mutations displayed comparable resistance levels to GS-9160 and GS-9224, but different levels of resistance against RAL. In particular, L74M did not potentiate G140S resistance against RAL. In addition, while the triple mutant conferred a higher level of resistance than Q148K alone against GS-9224 and GS-9160, it conferred a lower level of resistance than Q148K alone against RAL.

GS-9224 exhibits improved *in vitro* ADME properties compared to GS-9160

GS-9224 displayed a longer half-life than GS-9160 in human and dog hepatic microsomal extracts (Table 7). In addition, GS-9224 did not demonstrate any significant inhibition or induction of human CYP450 isoforms within clinically achievable range of concentrations (data not shown). When permeability was measured across a monolayer of Caco-2 cells, GS-9224 displayed higher permeability than GS-9160 in both apical to baso-lateral and baso-lateral to apical directions with a lower efflux ratio than GS-9160 or RAL (Table 7). Finally, the assessment of plasma protein binding by equilibrium dialysis against dog and human plasma showed that GS-9224 is more highly protein bound than GS-9160 both in dog plasma (~99.5% vs. ~93.5%) and in human plasma (~97.7% vs. ~89.6%) (Table 7).

Similar to GS-9160, GS-9224 is not metabolized by CYP450 enzymes in microsomes or hepatocytes but undergoes significant metabolic modification via glucuronidation. A study was carried

Compounds[d]	EC_{50} (nM)	Fold-Change in EC_{50} Relative to HIV-1 IIIb				
	HIV-1 IIIb	L74M[a]	G140S[b]	Q148K[c]	L74M/ G140S	L74M/ G140S/ Q148K
RAL	4.3	1.7	2	136	3	32
GS-9160	1.7	1	6	28	19	455
GS-9224	5.6	1	6	42	11	118

> 2-fold > 10-fold > 50-fold > 100-fold

[a] Selected by GS-9224 (this report), L-708,906 (32), S-1360 (33), L-870,810 (42) and GS-9160 (19).
[b] Selected by GS-9224 (this report) and L-Chicoric acid (29).
[c] Selected by GS-9224 (this report), S-1360 (31) and RAL (14, 39).
[d] The EC_{50} and fold-change represent the mean of a least two independent experiments performed in triplicate.

Table 6: Resistance Profile of Mutant Viruses Selected by GS-9224.

Compound	Liver Microsomal Stability[a] $T_{1/2}$ (min)		Cellular Permeability in Caco-2 Cells[b]			Plasma Protein Binding[c] (% Bound at 2 μM)	
	Dog	Human	P_{app} A→B (cm/sec × 10^{-6})	P_{app} A→B (cm/sec × 10^{-6})	Efflux Ratio	Dog	Human
RAL	353.9	257.1	2.8	9.5	3.4	—	—
GS-9160	43.6	26.5	1.6	6.0	3.8	93.5	89.6
GS-9224	67.1	30.2	3.8	8.8	2.3	99.5	97.7

[a] Mean of 13 independent experiments.
[b] Mean of 2 independent experiments.
[c] Mean of 3 determinations using equilibrium dialysis.

Table 7: *In Vitro* ADME Profiling of GS-9224 Relative to GS-9160 and RAL.

UGT Isoform	Gucuronidation Rate[a,b] (pmol/min/mg)										
	1A1	1A3	1A4	1A6	1A7	1A8	1A9	2B4	2B7	2B15	2B17
GS-9160	16.7	17.5	0.2	1.5	<0.02	1.9	1.9	<0.02	<0.02	<0.02	0.1
GS-9224	75.4	32.0	<0.02	<0.02	<0.02	1.6	1.3	<0.02	<0.02	0.2	<0.02[b]

[a] Mean of duplicate test.
[b] The Limit of rate detection is 0.02 pmol/min/mg.

Table 8: Rate of Glucuronidation of GS-9224 by Major UGT Isoforms.

out to determine the specific uridine diphosphate transferase (UGT) isoforms responsible for the metabolism of GS-9224. The results showed that UGT 1A1 and 1A3 are the main UGT isoforms responsible for glucuronidation of both GS-9160 and GS-9224 (Table 8). The characterization of GS-9224 metabolites formed systemically both *in vitro* and *in vivo* suggests the formation of a single phenolic glucuronide metabolite of GS-9224 (Figure 3).

Single-dose pharmacokinetics in healthy human subjects

After administration of single doses of GS-9224, 50 or 100 mg as an oral solution in the fasted state, maximum mean (CV%) concentrations of 110 ng/mL (51%) and 215 ng/mL (41%) were achieved at the 0.75 hour nominal time point, thereafter falling to <1.0 ng/mL in 8/8 (100%) and 7/8 (87.5%) subjects by the 12 hour time point for the 50 mg and 100 mg dose group, respectively. These data indicated rapid plasma elimination of GS-9224, consistent with a ~1.0 hour terminal elimination half-life that was incompatible with a goal of once-daily dosing. The free fraction (%fp) of GS-9224 in plasma samples collected after administration of 50 mg and 100 mg GS-9224 was 7.66 ± 1.25% and 9.44 ± 3.86% (mean ± SD), respectively.

Single doses of GS-9224 50 mg and 100 mg were safe and well tolerated in healthy, adult, male and female subjects. No discontinuations due to adverse events or serious adverse events occurred. All adverse events were mild with the exception of moderate diarrhea, vomiting, and headache in 1 subject. Headache, upper abdominal pain, diarrhea, and stomach discomfort (1 report of each) were each considered by the investigator to be related to study treatment.

Discussion

GS-9224 is an analog of GS-9160, a previously reported investigational INSTI [19]. GS-9224 was designed in an effort to optimize the pharmacokinetic profile of GS-9160 while retaining its antiviral potency. The medicinal chemistry optimization focused primarily on the p-fluorobenzyl moiety of GS-9160. Profiling of various analogs led to the identification of GS-9224 that differs structurally from GS-9160 by the addition of one chlorine atom and one fluorine atom on the p-fluorobenzyl moiety (Figure 1) [22].

Similar to GS-9160, GS-9224 exhibits potent and selective antiviral activity against HIV-1 and acts as an efficacious inhibitor of the IN strand transfer activity in an *in vitro* biochemical enzymatic assay. The elevation of 2-LTR circles in HIV-infected cells treated with GS-9224 was indicative of the inhibition of proviral DNA integration. In addition, GS-9224 profoundly reduced the number of integration events in treated cells as measured by Alu-LTR quantification of integration junctions without alteration of total viral DNA synthesis measured by the late-RT signal, demonstrating that GS-9224 is an authentic inhibitor of HIV-1 integration.

GS-9224 showed synergistic antiviral effect when combined with approved HIV drugs from different antiretroviral classes and retained antiviral potency against NRTI-, NNRTI- and PI-resistant HIV-1

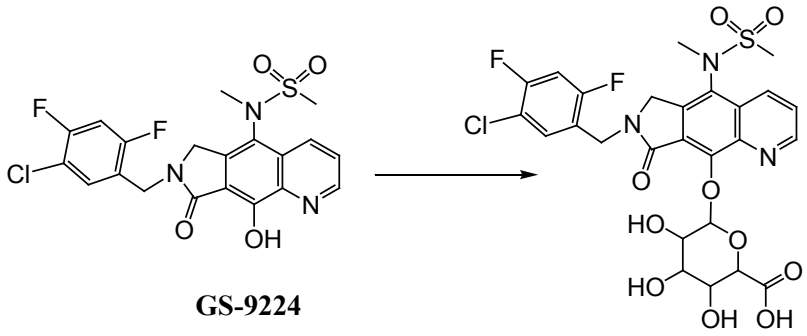

Figure 3: Phenolic glucuronide metabolite of GS-9224.

mutants, an observation consistent with its established mechanism of action. Characterizing the activity against a series of viruses expressing various INSTI resistance mutations revealed a similar resistance profile for GS-9224 and GS-9160. In comparison with RAL, both compounds showed lower degree of resistance against clinically relevant mutation Q148K, but higher level of resistance against E92Q and N155H mutants observed in patients treated with either RAL or EVG [44,45].

In vitro passaging of HIV-1 in the presence of gradually increasing concentrations of GS-9224 resulted in the selection of an IN mutant variant with >100-fold resistance to the selecting inhibitor and a similar cross-resistance to other INSTIs including RAL and the parent inhibitor GS-9160. Clonal sequencing of the resistant variant revealed the emergence of G140S and L74M mutations followed by the Q148K mutation. It is interesting to note that Q148K emerged as a primary mutation in patients treated with RAL who experienced virologic failure [3,4], but in the selection with GS-9224, Q148K emerged only after L74M and G140S. Thus, it appears that Q148K is a secondary mutation that augments resistance of L74M/G140S against GS-9224. In contrast, Q148K displays a higher degree of resistance to RAL as a primary single mutation compared to the triple mutant L74M/G140S/Q148K selected by GS-9224.

The additional chlorine and fluorine atoms on the fluorobenzyl moiety of GS-9160 conferred to GS-9224 a moderately higher hepatic microsome stability, better absorption potential, lower efflux ratio and higher serum protein binding compared to GS-9160 (Table 7).

In healthy human subjects, GS-9224 rapidly achieved maximum plasma concentrations within one hour of administration as a solution in the fasted state. Thereafter, concentrations rapidly declined with a terminal elimination half-life of ~1.0 hour. These human pharmacokinetic results were inconsistent with the target pharmacokinetic profile to provide sustained, therapeutic concentrations over a 24 hour dosing interval. As such, from a clinical pharmacology perspective, GS-9224 was deemed not suitable for QD dosing. In these clinically derived samples, the mean free fraction of GS-9224 was 7.5 to 10%, indicating lower *in vivo* protein binding than that estimated from *in vitro* plasma equilibrium dialysis for both dogs and humans. This could, at least in part, contribute to the fast systemic elimination of GS-9224 in humans. Single doses of GS-9224 at 50 mg and 100 mg were safe and well tolerated in healthy, adult, male and female subjects.

In conclusion, GS-9224 has retained the antiviral potency, mechanism of action and resistance profile of the predecessor compound, GS-9160. In addition, it exhibited improved in vitro ADME profile including higher metabolic stability, absorption potential and serum protein binding. However, these differential properties did not translate into an improved pharmacokinetic profile in healthy human volunteers. Results from the assessment of the single-dose pharmacokinetics revealed a profile of GS-9224 that would not be compatible with the once-daily oral dosing of GS-9224 due to faster than expected systemic elimination of the drug.

Acknowlegments

The authors thank Richard Pastor, Sammy Metobo, Rachael Lansdown and Salman Jabri for synthesizing.

References

1. DeJesus E, Berger D, Markowitz M, Cohen C, Hawkins T, et al. (2006) Antiviral activity, pharmacokinetics, and dose response of the HIV-1 integrase inhibitor GS-9137 (JTK-303) in treatment-naïve and treatment-experienced patients. J Acquir Immune Defic Syndr 43:1-5.
2. Markowitz M, Morales-Ramirez JO, Nguyen B-Y, Kovacs CM, Steigbigel RT, et al. (2006) Antiretroviral activity, pharmacokinetics, and tolerability of MK-0518, a novel inhibitor of HIV-1 integrase, dosed as monotherapy for 10 Days in treatment-naïve HIV-1–infected individuals. J Acquir Immune Defic Syndr 43: 509-515.
3. Cooper DA, Steigbigel RT, Gatell JM, Rockstroh JK, Katlama C, et al. (2008) Subgroup and resistance analyses of raltegravir for resistant HIV-1 infection. N Engl J Med 359: 355-365.
4. Steigbigel RT, Cooper DA, Kumar PN, Eron JE, Schechter M, et al. (2008) Raltegravir with optimized background therapy for resistant HIV-1 infection. N Engl J Med 359: 339-354.
5. Markowitz M, Nguyen B-Y, Gotuzzo E, Mendo F, Ratanasuwan W, et al. (2009) Sustained antiretroviral effect of raltegravir after 96 weeks of combination therapy in treatment-naive patients with HIV-1 infection. J Acquir Immune Defic Syndr 52: 350-356.
6. Zolopa AR, Berger DS, Lampiris H, Zhong L, Chuck SL, et al. (2010) Activity of elvitegravir, a once-daily integrase inhibitor, against resistant HIV Type 1: results of a phase 2, randomized, controlled, dose-ranging clinical trial. J Infect Dis 201**:** 814–822.
7. Xu L, Liu H, Hong A, Vivian R, Murray BP, et al. (2014) Structure-activity relationships of diamine inhibitors of cytochrome P450 (CYP) 3A as novel pharmacoenhancers. Part II: P2/P3 region and discovery of cobicistat (GS-9350) Bioorg Med Chem Lett 24: 995-999.
8. Shimura K, Kodama EN (2009) Elvitegravir: a new HIV integrase inhibitor. Antivir. Chem Chemother 20: 79-85.
9. Sax PE, DeJesus E, Mills A, Zolopa A, Cohen C, et al. (2012) Co-formulated elvitegravir, cobicistat, emtricitabine, and tenofovir versus co-formulated efavirenz, emtricitabine, and tenofovir for initial treatment of HIV-1 infection: a randomised, double-blind, phase 3 trial, analysis of results after 48 weeks. Lancet 379: 2439-2448.
10. DeJesus E, Rockstroh J, Henry K, Molina JM, Gathe J, et al. (2012) Co-formulated elvitegravir, cobicistat, emtricitabine, and tenofovir disoproxil fumarate versus ritonavir-boosted atazanavir plus co-formulated emtricitabine and tenofovir disoproxil fumarate for initial treatment of HIV-1 infection: a randomised, double-blind, phase 3, non-inferiority trial. Lancet **379:** 2429-2438.

11. Rockstroh JK, DeJesus E, Henry K, Molina JM, Gathe J, et al. (2013) A randomized, double-blind comparison of co-formulated elvitegravir/cobicistat/emtricitabine/ tenofovir versus ritonavir-boosted atazanavir plus co-formulated emtricitabine and tenofovir DF for initial treatment of HIV-1 infection: analysis of week 96 results. J Acquir Immune Defic Syndr 62: 483-486.

12. Zolopa A, Sax PE, DeJesus E, Mills A, Cohen C, et al. (2013) A randomized, double-blind comparison of co-formulated elvitegravir/cobicistat/emtricitabine/ tenofovir DF versus efavirenz/emtricitabine/ tenofovir DF for initial treatment of HIV-1 infection: analysis of week 96 results. J Acquir Immune Defic Syndr 63: 96-100.

13. Garrido C, Villacian J, Zahonero N, Pattery T, Garcia F, et al. (2012) Broad phenotypic cross-resistance to elvitegravir in HIV-infected patients failing on raltegravir-containing regimens. Antimicrob Agents Chemother 56: 2873-2878.

14. Hazuda DJ, Anthony NJ, Gomez RP, Jolly SM, Wai JS, et al. (2004) A naphthyridine carboxamide provides evidence for discordant resistance between mechanistically identical inhibitors of HIV-1 integraseProc Natl Acad Sci U S A 101: 11233-11238.

15. Malet I, Delelis O, Valantin M-A, Montes B, Soulie C, et al. (2008) Mutations associated with failure of raltegravir treatment affect integrase sensitivity to the inhibitor in vitro. Antimicrob Agents Chemother 52: 1351-1358.

16. Min S, Song I, Borland J, Chen S, Lou Y, et al. (2010) Pharmacokinetics and safety of S/GSK1349572, a next generation HIV integrase inhibitor, in healthy volunteers. Antimicrob. Agents Chemother. 54: 254-258.

17. Kobayashi M, Yoshinaga T, Seki T, Wakasa-Morimoto C, Brown KW, et al. (2011) In Vitro antiretroviral properties of S/GSK1349572, a next-generation HIV integrase inhibitor. Antimicrob. Agents Chemother. 55:813–821.

18. Raffi F, Rachlis A, Stellbrink HJ, Hardy WD, Torti C, et al. (2013) Once-daily dolutegravir versus raltegravir in antiretroviral-naive adults with HIV-1 infection: 48 week results from the randomised, double-blind, non-inferiority SPRING-2 study. Lancet 381: 735-743.

19. Jones GS, Yu F, Zeynalzadegan A, Hesselgesser J, Chen X, et al. (2009) Preclinical evaluation of GS-9160, a novel inhibitor of human immunodeficiency virus type 1 integrase. Antimicrob Agents Chemother 53: 1194-1203.

20. Jin H, Cai RZ, Schacherer L, Jabri S, Tsiang M, et al. (2006) Design, synthesis, and SAR studies of novel and highly active tri-cyclic HIV integrase inhibitors. Bioorg Med Chem Lett 16: 3989-3992.

21. Jin H, Wright M, Pastor R, Mish M, Metobo S, et al. (2008) Tricyclic HIV integrase inhibitors: potent and orally bioavailable C5-aza analogs. Bioorg Med Chem Lett 18: 1388-1391.

22. Jin H, Metobo S, Jabri S, Mish M, Lansdown R, et al. (2009) Tricyclic HIV integrase inhibitors V. SAR studies on the benzyl moiety. Bioorg Med Chem Lett 19: 2263-2265.

23. Cihlar T, Ray AS, Boojamra CG, Zhang L, Hui H, et al. (2008) Design and profiling of GS-9148, a novel nucleotide analog active against nucleoside-resistant variants of human immunodeficiency virus type 1, and its orally bioavailable phosphonoamidate prodrug, GS-9131. Antimicrob. Agents Chemother. 52: 655-665.

24. Cihlar T, He GX, Liu X, Chen JM, Hatada M, et al. (2006) Suppression of HIV-1 protease inhibitor resistance by phosphonate-mediated solvent anchoring. J Mol Biol 363: 635-647.

25. Yu F, Jones GS, Hung M, Wagner AH, MacArthur HL, et al. (2007) HIV-1 integrase preassembled on donor DNA is refractory to activity stimulation by LEDGF/p75. Biochemistry 46: 2899-2908.

26. Butler SL, Hansen MST, Bushman FD (2001) A quantitative assay for HIV DNA integration in vivo. Nature Medicine 7: 631-634.

27. Kafri T, Van Praag H, Ouyang L, Gage FH, Verma IM (1999) A packaging cell line for lentivirus vectors. J Virol 73: 576-584.

28. Bukrinsky M, Sharova N, Stevenson M (1993) Human Immunodeficiency Virus Type 1 2-LTR Circles Reside in a Nucleoprotein Complex Which Is Different from the Preintegration Complex. J Virol 67: 6863-6865.

29. King PJ, Robinson Jr. WE (1998) Resistance to the anti-human immunodeficiency virus type 1 compound L-chicoric acid results from a single mutation at amino acid 140 of integrase. J Virol 72: 8420-8424.

30. Hazuda DJ, Felock P, Witmer M, Wolfe A, Stillmock K, et al. (2000) Inhibitors of strand transfer that prevent integration and inhibit HIV-1 replication in cells. Science 287: 646-650.

31. Kobayashi M, Nakahara K, Seki T, Miki S, Kawauchi S, et al. (2008) Selection of diverse and clinically relevant integrase inhibitor-resistant human immunodeficiency virus type 1 mutants. Antiviral Res. 80:213-222.

32. Fikkert V, Van Maele B, Vercammen J, Hantson A, Van Remoortel B, et al. (2003) Development of resistance against diketo derivatives of human immunodeficiency virus type 1 by progressive accumulation of integrase mutations. J Virol **77:** 11459-11470.

33. Fikkert V, Hombrouck A, Van Remoortel B, De Maeyer M, Pannecouque C, et al. (2004) Multiple mutations in human immunodeficiency virus-1 integrase confer resistance to the clinical trial drug S-1360. AIDS 18: 2019-2028.

34. Hazuda DJ, Young SD, Guare JP, Anthony NJ, Gomez RP, et al. (2004) Integrase inhibitors and cellular immunity suppress retroviral replication in rhesus macaques. Science 305: 528-532.

35. Shimura K, Kodama E, Sakagami Y, Matsuzaki Y, Watanabe W, et al. (2008) Broad antiretroviral activity and resistance profile of the novel human immunodeficiency virus integrase inhibitor elvitegravir (JTK-303/GS-9137) J Virol 82: 764-774.

36. Low A, Prada N, Topper M, Vaida F, Castor D, et al. (2009) Natural polymorphisms of human immunodeficiency virus type 1 integrase and inherent susceptibilities to a panel of integrase inhibitors. Antimicrob Agents Chemother. 53:4275-4282.

37. Margot NA, Hluhanich RM, Jones GS, Andreatta KN, Tsiang M, et al. (2012) In vitro resistance selections using elvitegravir, raltegravir, and two metabolites of elvitegravir M1 and M4. Antiviral Res 93: 288-296.

38. Abram ME, Hluhanich RM, Goodman DD, Andreatta KN, Margot NA, et al. (2013) Impact of primary elvitegravir resistance-associated mutations in HIV-1 integrase on drug susceptibility and viral replication fitness. Antimicrob. Agents Chemother. 57: 2654-2663.

39. Fransen S, Gupta S, Danovich R, Hazuda D, Miller M, et al. (2009) Loss of raltegravir susceptibility by human immunodeficiency virus type 1 is conferred via multiple nonoverlapping genetic pathways. J Virol 83: 11440-11446.

40. Eron JJ, Cooper DA, Steigbigel RT, Clotet B, Gatell JM, et al. (2013) Efficacy and safety of raltegravir for treatment of HIV for 5 years in the BENCHMRK studies: final results of two randomised, placebo-controlled trials. Lancet Infect Dis 13: 587-596.

41. Steigbigel RT, Cooper DA, Teppler H, Eron JJ, Gatell JM, et al. (2010) Long-term efficacy and safety of Raltegravir combined with optimized background therapy in treatment-experienced patients with drug-resistant HIV infection: week 96 results of the BENCHMRK 1 and 2 Phase III trials Clin Infect Dis 50: 605-612.

42. Hombrouck A, Voet A, Van Remoortel B, Desadeleer C, De Maeyer M, et al. (2008) Mutations in HIV-1 integrase confer resistance to the naphthyridine L-870,810 and cross resistance to the clinical trial drug GS-9137. Antimicrob. Agents Chemother 52: 2069-2078.

43. Lataillade M, Chiarella J, Kozal MJ (2007) Natural polymorphism of the HIV-1 integrase gene and mutations associated with integrase inhibitor resistance. Antiviral Ther 12**:** 563-570.

44. Geretti AM, Armenia D, Ceccherini-Silberstein F (2012) Emerging patterns and implications of HIV-1 integrase inhibitor resistance. Curr Opin Infect Dis 25: 677-686.

45. Mesplède T, Quashie PK, Wainberg MA (2012) Resistance to HIV integrase inhibitors. Curr Opin HIV AIDS 7: 401-408.

Citation: Jones GS, Hluhanich R, Wieman LM, Zheng J, Huang W, et al. (2014) Preclinical and Clinical Profile of HIV-1 Integrase Strand-transfer Inhibitor GS-9224 Compared to its Parent Compound GS-9160. J Antivir Antiretrovir 6: 075-083. doi:10.4172/jaa.1000101